Frontiers in Bioscience Landmark

Front. Biosci. (Landmark Ed) **2023**; 28(7): 136
https://doi.org/10.31083/j.fbl2807136

Original Research

ER Stress is Activated and Involved in Disuse-Induced Muscle Atrophy

Lu Wang[1,2,†], Xiangsheng Pang[1,2,†], Shiming Li[2], Wenjiong Li[1], Xiaoping Chen[1,2,*], Peng Zhang[1,*]

[1]State Key Laboratory of Space Medicine Fundamentals and Application, China Astronaut Research and Training Center, 100094 Beijing, China
[2]National Key Laboratory of Human Factors Engineering, China Astronaut Research and Training Center, 100094 Beijing, China
*Correspondence: xpchen2009@163.com (Xiaoping Chen); zhangpeng6128@163.com (Peng Zhang)
[†]These authors contributed equally.

Academic Editors: Elisa Belluzzi and Graham Pawelec
Submitted: 16 December 2022 Revised: 9 February 2023 Accepted: 23 February 2023 Published: 13 July 2023

Abstract

Background: Muscle atrophy resulting wholly or partially from disuse represents a serious medical complication that decreases quality of life and increases morbidity and mortality. The accumulation of misfolded/unfolded proteins disrupts endoplasmic reticulum (ER) homeostasis and thus causes ER stress. Growing evidence indicates that ER stress plays an essential role in skeletal muscle remodeling under various physiological or pathophysiological conditions. However, whether ER stress is involved in disuse-induced muscle atrophy remains unclear. **Methods**: To induce muscle atrophy, 8-week-old C57BL/6JNifdc male mice were subjected to 3, 7, or 14 days of hindlimb unloading (HU), and rhesus macaques (*Macaca mulatta*) were subjected to 10° head-down tilted bed rest (HDBR) for 6 weeks. Tauroursodeoxycholic acid (TUDCA) (500 mg/kg/d) was orally administered to mice during HU to inhibit ER stress. Quantitative PCR, Western blotting, and immunohistochemistry were conducted to evaluate gene, protein, and structural changes, respectively. **Results**: ER stress marker genes were rapidly induced by HU in a similar trend to that observed with atrophy-related genes such as *Atrogin-1*, muscle RING finger 1 (*MuRF1*), and muscle ubiquitin ligase of SCF complex in atrophy-1 (*MUSA1*). Inhibition of ER stress with TUDCA, a pan-ER stress inhibitor, attenuated HU-induced muscle atrophy and the upregulation of ubiquitin ligases *via* the AKT/forkhead box O3a pathway. In addition, the oxidative-to-glycolytic myofiber type transition caused by HU was also inhibited by TUDCA treatment. ER stress activation was also confirmed in HDBR-induced rhesus soleus muscle atrophy. **Conclusions**: The strong positive correlation between ER stress activation and both HU- and HDBR-induced muscle atrophy indicates that ER stress activation is ubiquitously involved in disuse-induced muscle atrophy, regardless of species. Thus, inhibiting ER stress may be an effective therapeutic strategy to prevent muscle atrophy during disuse.

Keywords: disuse; muscle atrophy; ER stress; hindlimb unloading; head-down tilted bed rest

1. Introduction

Skeletal muscle is the largest organ of the human body, accounting for almost 40% of the total body weight. The mass and myofiber type composition of skeletal muscle are essential for its functions, including postural control, exercise, and metabolism [1]. However, prolonged periods of disuse, such as those occurring during spaceflight, bed rest, hindlimb unloading (HU), and immobilization or denervation, induce significant muscle atrophy, with the greatest loss of muscle mass observed in antigravity muscles (e.g., the soleus muscle) [2–4]. In addition, disuse-induced muscle atrophy is accompanied by a transition from oxidative (type I and IIa myosin heavy chain isoforms, MyHC-I and MyHC-IIa, respectively) to glycolytic (type IIx and IIb myosin heavy chain isoforms, MyHC-IIx and MyHC-IIb, respectively) myofiber type [2,3]. Consequently, disuse-induced muscle atrophy leads to weakness, reduces whole-body insulin sensitivity, and increases the risk of falls and mortality [2,4]. Despite these broad negative impacts on human health, the molecular mechanisms responsible for disuse-induced muscle atrophy are not well understood.

As a dynamic tissue, skeletal muscle undergoes extensive adaptations in response to a large variety of stimuli [1]. One of the main structural components involved in the rapid skeletal muscle response to environmental changes is the highly developed endoplasmic reticulum (ER) [5,6]. The ER plays a pivotal role in protein folding, the structural maturation of cellular proteins, and calcium homeostasis [7]. However, the accumulation of misfolded and unfolded proteins, caused by environmental or genetic factors, can ultimately lead to stress in the ER lumen. In response to stress and to restore ER homeostasis, cells initiate the unfolding protein response (UPR). The UPR is mediated by three major ER-resident stress sensors: inositol-requiring protein 1 (IRE-1), protein kinase R-like ER kinase (PERK), and activating transcription factor 6 (ATF-6) [8]. Binding immunoglobulin protein (BiP), one of the most abundant ER chaperones, dissociates from these three sensors upon stress, leading to their activation through either oligomerization or export. Activated PERK phosphorylates eukaryotic initiation factor 2 (eIF2), which increases the translation of ATF4 and expression of stress-responsive genes such as C/EBP homologous protein (CHOP) [8]. The endori-

Copyright: © 2023 The Author(s). Published by IMR Press.
This is an open access article under the CC BY 4.0 license.

Publisher's Note: IMR Press stays neutral with regard to jurisdictional claims in published maps and institutional affiliations.

bonuclease activity of IRE-1α cleaves a 26-base-pair segment from Xbox-binding protein 1 (Xbp1) mRNA, creating an alternative mRNA that is translated into the active (or spliced) form of the transcription factor Xbp1 (Xbp1s) [8]. ATF6 translocates to the nucleus where it acts as a transcription factor to regulate target gene expression. Together, these pathways work to decrease translation and increase protein folding to alleviate ER stress. If these pathways fail, a cell death program is triggered [8].

Accumulating evidence has highlighted the essential role of ER stress and the UPR pathway in skeletal muscle remodeling under various conditions [9–11]. ER stress is activated in skeletal muscle by exercise and regulates exercise-induced adaptations through the peroxisome proliferator-activated receptor gamma coactivator-1α/ATF6α complex [12]. In some catabolic states (e.g., cachexia), ER stress and UPR pathways are activated and thought to be involved in the maintenance of skeletal muscle mass and strength [13]. Several studies have reported changes in the expression of ER stress markers in disuse-induced muscle atrophy, but these results have not been consistent and have even been contradictory in some instances. For example, *BiP* was decreased and *IRE1* and *PERK* were increased in the unloaded rat soleus muscle [14], whereas some studies showed no significant changes in the expression of BiP and CHOP in the rat soleus muscle after HU [15,16]. In the gastrocnemius muscle of mice, *BiP*, *ATF4*, *CHOP*, and *Xbp1s* were upregulated by HU [17]. Thus, the exact role of ER stress in disuse-induced muscle atrophy still remains to be elucidated.

In this study, we examined changes of ER stress markers in the soleus muscle for different periods of HU. Our results showed that most ER stress components were upregulated in a trend similar to atrophy-related genes, showing close association with muscle atrophy. Inhibition of ER stress alleviated HU-induced muscle atrophy and concomitant myofiber type transition. ER stress activation was confirmed in head-down tilted bed rest (HDBR)-induced rhesus soleus muscle atrophy. These data suggest that ER stress activation mediates disuse-induced muscle atrophy and inhibiting ER stress represents an attractive therapeutic strategy in combating this muscle wasting disorder.

2. Materials and Methods

2.1 Mice and HU

Male C57BL/6JNifdc mice (8 weeks old) were obtained from Vital River Laboratories (Beijing, China) and acclimatized to their new surroundings for 1 week before the start of the study. To induce HU, mice were elevated sufficiently to prevent their hindlimbs from touching the cage floor or sides for 3, 7, or 14 days as previously described [18]. To inhibit ER stress, tauroursodeoxycholic acid (TUDCA) (500 mg/kg body weight) was administered daily by gavage during the 14 days of HU [19], as it has been demonstrated to display potential therapeutic benefits in various models of many diseases at this dose [20–22]. Control mice were given an equal volume of vehicle (phosphate-buffered saline [PBS]). At the end of the experimental periods, hindlimb muscles were immediately removed, weighed, and frozen in liquid nitrogen or embedded in tissue-freezing medium for subsequent morphological and immunohistochemical analyses. All animal procedures were conducted in accordance with standard ethical guidelines and approved by the Institutional Animal Care and Use Committee of the China Astronaut Research and Training Center (ACC-IACUC-2021-021).

2.2 Rhesus Macaques and HDBR

A total of nine healthy male rhesus macaques, aged 5–7 years and weighing 9–10 kg, were purchased from the Beijing Institute of Xie'erxin Biology Resource (Beijing, China). The animals were acclimatized for 3 months including preliminary caretaker handling, confinement jacket fitting, and tilt-table acclimation training at the Laboratory Animal Center of the China Astronaut Research and Training Center prior to being used in experiments. The rhesus macaques were randomly divided into control (n = 3) and 42-day HDBR groups (n = 6) with matching weights. Rhesus macaques in the HDBR group were subjected to 42 days of –10° HDBR as previously described [23]. At the end of the 42-day HDBR experiment, approximately 100 mg muscle was harvested from the belly of the soleus muscle for subsequent analyses. All procedures were performed in accordance with the standard ethical guidelines and approved by the Institutional Animal Care and Use Committee of the China Astronaut Research and Training Center (ACC-IACUC-2019-002).

2.3 RNA Extraction and Quantitative PCR

For each muscle sample, total RNA was extracted with TRIzol according to the manufacturer's instructions (15596-026; Invitrogen, Carlsbad, CA, USA). The PrimeScript RT Reagent Kit (RR037A; Takara, Shiga, Japan) was used to reverse transcribe total RNA (500 ng) into complementary DNA according to the manufacturer's instructions. Quantitative PCR (qPCR) was performed in triplicate using the StepOnePlus Realtime PCR System (4376357; Invitrogen). Each PCR mixture (final reaction volume 50 µL) contained 21 µL sterile water, 25 µL SYBR Green (4309155; Invitrogen), 2 µL cDNA (50 ng/µL), 1 µL forward primer (10 pmol/µL), and 1 µL reverse primer (10 pmol/µL). PCR was performed with initial denaturation at 95 °C for 10 min, followed by 40 cycles of 95 °C for 10 s, 62 °C for 15 s, and 72 °C for 20 s. Gene amplification was performed according to a melting program of 70 °C for 15 s, and fluorescence was monitored continuously during the change in temperature from 60 °C to 95 °C at 0.3 s. Target gene expression levels were calculated to that of the *18S* rRNA gene and normalized to the control group. Experiments were repeated at least three times. The primer sequences are listed in **Supplementary Tables 1** and **2**.

2.4 Immunoblotting

Skeletal muscle was homogenized in lysis buffer (in mM) containing: 25 Tris-HCl (pH 7.6), 150 NaCl, 1 EDTA, 1% Triton X-100, 10% glycerol, and 1% protease inhibitor cocktail. Supernatants were collected, and the protein concentration was determined using Bradford protein assay reagents (500-0203; Bio-Rad, Hercules, CA, USA). Equal amounts of extracted proteins (30 µg per lane) were denatured in sodium dodecyl sulfate (SDS) loading buffer and separated on SDS-polyacrylamide gels. Proteins were electrotransferred to a nitrocellulose membrane. The membranes were blocked in 5% nonfat milk or bovine serum albumin (BSA) for 1 h and then incubated overnight at 4 °C with primary antibodies against phospho-IRE1α (S724) (ab288371; Abcam, Cambridge, MA, USA), CHOP (5554; Cell Signaling Technology [CST], Danvers, MA, USA), ATF4 (11815; CST), BiP (3177S; CST), phospho-AKT (Ser473) (4060S; CST), AKT (pan) (4691S; CST), forkhead box O3a (FoxO3a) (2497S; CST), Atrogin-1 (MP2041; ECM Biosciences, Versailles, KY, USA), muscle RING finger 1 (MuRF1) (MP3401; ECM Biosciences), troponin I, slow skeletal type (Tn I-SS) (ARP42117-P050; Aviva Systems Biology, San Diego, CA, USA), Tn I-FS (11634-1-AP; Proteintech, Rosemont, IL, USA), and β-actin (sc-47778; Santa Cruz, Dallas, TX, USA). Signals were visualized on X-ray film or an imaging system (4800 Multi; Tanon, Shanghai, China) by incubating membranes with horse radish peroxidase-coupled secondary antibodies and enhanced chemiluminescence reagent (Prod34080; Thermo Fisher Scientific, Waltham, MA, USA). Blots were stripped with stripping reagent (21059; Thermo Fisher Scientific) according to the manufacturer's instructions and reprobed if necessary. Proteins were quantified using Image-Pro Plus Version 6.0 (Media Cybernetics, Rockville, MD, USA), and the strength of each protein signal was normalized to the corresponding β-actin signal. Data are expressed as percent expression compared to the control group.

2.5 Immunostaining

Cryosections of soleus muscle were fixed in 4% paraformaldehyde for 10 min at 4 °C and washed with PBS. After incubating for 30 min with 0.3% Triton X-100, sections were blocked for 1 h in 5% goat serum. The cross-sectional area (CSA) of soleus muscle fibers was determined by immunostaining with anti-laminin antibody (ab11575; Abcam). To distinguish different myofiber types, soleus muscle sections were double-immunostained by combining rabbit-anti-laminin with one of the following antibodies (all from Hybridoma Bank, Iowa City, IA, USA): BA-D5 that recognizes the MyHC-I isoform, SC-71 for the MyHC-IIa isoform, 6H1 for the MyHC-IId isoform, or BF-F3 for the MyHC-IIb isoform. Primary antibodies were detected with Alexa Fluor® 594 (A11012; Invitrogen) fluorescent dye conjugated to an anti-rabbit secondary antibody or Alexa Fluor® 488 (A11001; Invitrogen) fluorescent dye conjugated to an anti-mouse secondary antibody. Fiber CSA and the number of fibers immunostained with the above-mentioned different MyHC isoforms were calculated using Image-Pro Plus 6.0.

2.6 Statistical Analyses

Data are presented as the mean ± standard deviation (SD). The two-tailed unpaired *t*-test was used for comparisons between two groups, and multigroup comparisons were analyzed using one-way analysis of variance followed by Bonferroni post-hoc test using GraphPad Prism version 7.0 (GraphPad Software, Inc., La Jolla, CA, USA). Pearson's correlation analysis was performed to assess the correlation between two variables.

3. Results

3.1 ER Stress is Activated in HU-Induced Muscle Atrophy

To elucidate the role of ER stress in disuse-induced muscle atrophy, a time course of changes in ER stress markers in the soleus muscle of mice was determined in response to HU. As expected, the soleus muscle displayed the greatest muscle mass loss during HU compared to other hindlimb muscles (Fig. 1A). Atrophy-related genes including *Fbxo32* (*atrogin-1*), *Trim63* (*MuRF1*), and *Fbxo30* (*MUSA1*) were induced after 3 days of HU and reached their highest expression after 7 days of HU (Fig. 1B). Of the nine ER stress marker genes measured, four (*PERK*, *IRE1*α, *ATF4,* and *CHOP*) were significantly upregulated after 3 days of HU, and five (*ATF4*, *CHOP*, *Xbp1u*, *Xbp1s*, and *BiP*) reached their highest expression levels at 7 days of HU, showing similar expression patterns to those observed with atrophy-related genes (Fig. 1C).

To confirm the correlation between ER stress and muscle atrophy, a correlation assay was performed between the relative expression of ER stress markers and the loss of soleus muscle mass during HU. As shown in Fig. 1D, four of the nine ER stress markers (*ATF4*, *growth arrest* and *DNA damage-inducible protein 34*, *Xbp1s*, and *BiP)* were positively correlated with the loss of soleus muscle mass caused by HU. These data indicate that ER stress is significantly activated by HU and may contribute to HU-induced muscle atrophy.

3.2 Inhibition of ER Stress Alleviates Disuse-Induced Muscle Atrophy via Regulation of the AKT/FoxO3a Pathway

To determine whether the ER mediates disuse-induced muscle atrophy, the effect of ER stress inhibition on HU-induced muscle atrophy was determined. TUDCA, a pan-ER stress inhibitor, was used to inhibit HU-induced ER stress activation (Fig. 2A). HU resulted in significant loss of soleus muscle mass in vehicle-treated mice, which was less evident in TUDCA-treated mice (Fig. 2B). Anti-laminin immunostaining analysis clearly delineated a decrease in

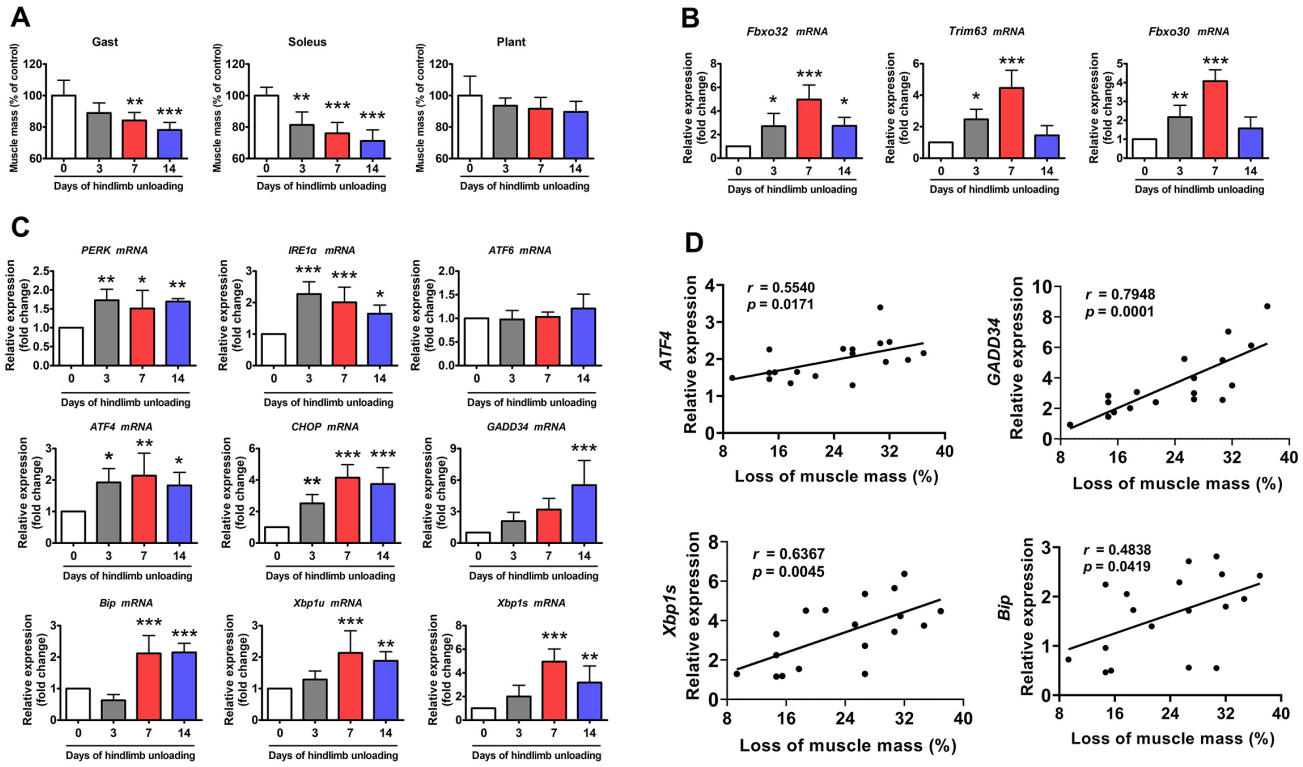

Fig. 1. ER stress was activated in the soleus muscle of mice during HU. (A) Changes in skeletal muscle mass during 14 days of HU (n = 6). Gast, gastrocnemius; Plant, plantaris. (B) qPCR analysis of *Fbxo32, Trim63* and *Fbxo30* in the soleus muscle of mice during 14 days of HU (n = 6). (C) qPCR analysis of the indicated ER stress marker genes in the soleus muscle of mice during 14 days of HU (n = 6). (D) Correlation between the expression of ER stress marker genes and loss of soleus muscle mass. Regression lines are displayed. r, correlation coefficient. Pearson's correlation analysis was used to determine the correlations. Data are shown as the mean ± SD. *$p < 0.05$, **$p < 0.01$, ***$p < 0.001$ vs. the control (0) group by one-way analysis of variance.

myofiber CSA in unloaded soleus muscle, indicative of severe myofiber atrophy (Fig. 2C). By contrast, TUDCA treatment attenuated the reduction in myofiber CSA caused by HU (Fig. 2C). Western blot analysis showed the marked upregulation of Atrogin-1 and MuRF1 in unloaded soleus muscle (Fig. 2D). This upregulation was significantly reduced in TUDCA-treated mice (Fig. 2D), which further confirmed the inhibitory effect of TUDCA on HU-induced muscle atrophy.

Because AKT/FoxO3a is a key signaling pathway that regulates the expression of atrophy-related genes, we next determined whether the inhibition of ER stress with TUDCA affected the activity of the AKT/FoxO3a pathway during HU-induced muscle atrophy. Western blotting showed that the levels of phosphorylated AKT (Ser473) (p-AKT) were decreased and those of FoxO3a were increased in the soleus muscle of vehicle-treated mice after HU (Fig. 2D). However, treatment with TUDCA restored the expression of p-AKT and decreased the expression of FoxO3a in unloaded soleus muscle (Fig. 2D), suggesting that TUDCA inhibited HU-induced muscle atrophy by regulating the AKT/FoxO3a pathway.

3.3 Inhibition of ER Stress Attenuates Disuse-Induced Myofiber Type Transition

Disuse-induced muscle atrophy is characterized by oxidative-to-glycolytic myofiber type transition. Thus, the effect of ER stress inhibition on HU-induced myofiber type transition was determined. As shown in Fig. 3A, HU markedly downregulated the mRNA expression of *MyHC-IIa* and upregulated the mRNA expression of *MyHC-IIx* and *MyHC-IIb*. Immunostaining for MyHC isoforms in unloaded soleus muscle sections also exhibited a reduced proportion of MyHC-IIa isoform and an increased proportion of MyHC-IIb isoform with HU (Fig. 3B). TUDCA treatment partially prevented the downregulation of MyHC-IIa and the upregulation of MyHC-IIb caused by HU (Fig. 3A,B). Protein expression of slow-twitch troponin (Tn I-SS) and fast-twitch troponin (Tn I-FS) in the soleus muscles was also determined by western blotting. Tn I-SS was decreased, and Tn I-FS was increased after 14 days of HU in vehicle-treated mice, and these changes were attenuated in TUDCA-treated mice (Fig. 3C). Collectively, these results suggested that inhibition of ER stress with TUDCA prevented the myofiber type transition caused by HU.

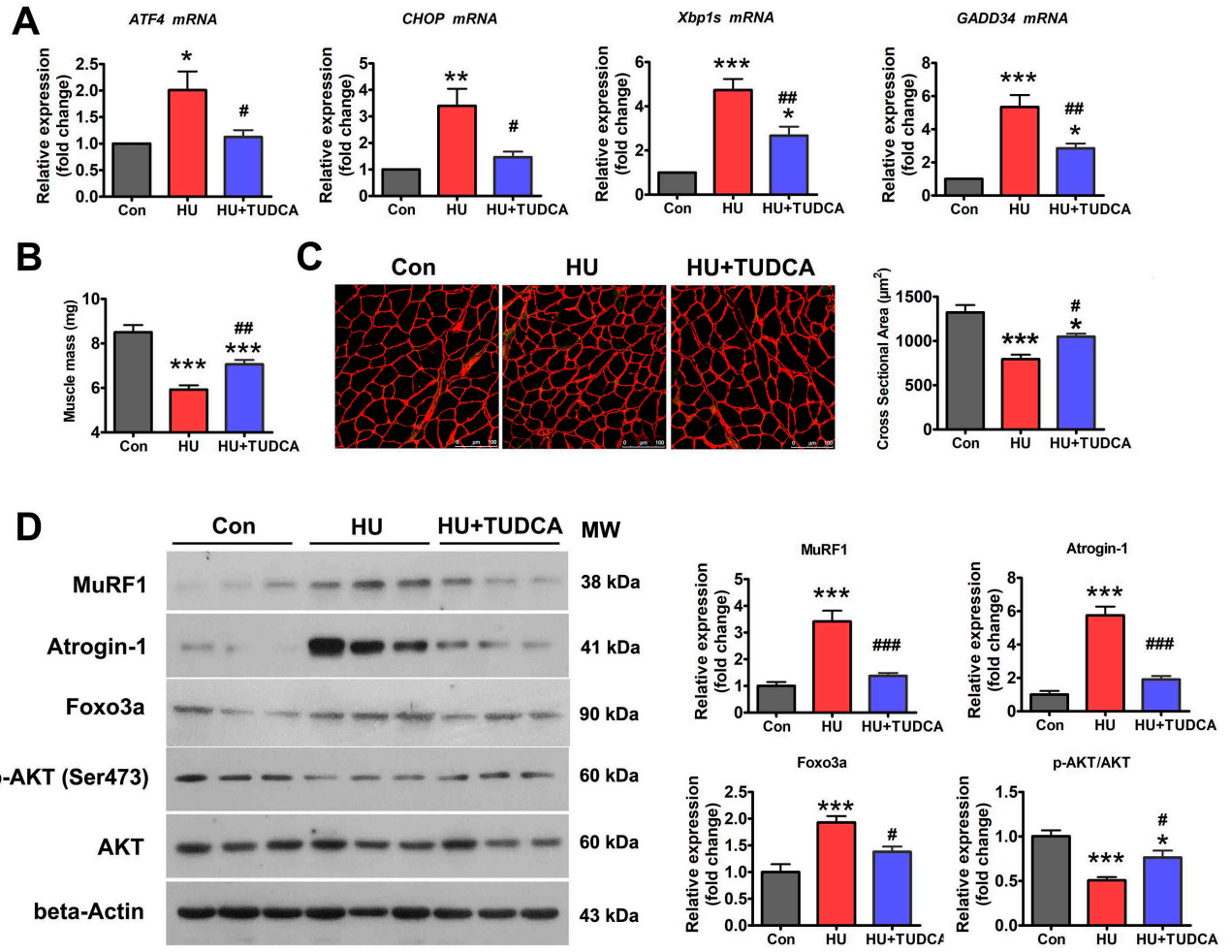

Fig. 2. TUDCA inhibited HU-induced muscle atrophy *via* regulation of the p-AKT/FoxO3a pathway. (A) qPCR analysis of the indicated ER stress markers in the soleus muscle of control, HU, and HU+TUDCA mice (n = 5). (B) Soleus muscle mass from control, HU, and HU+TUDCA mice (n = 10). (C) Representative immunostaining for laminin in the soleus muscle cross-sections of control, HU, and HU+TUDCA mice and quantification of CSA (n = 4). Scale bars: 100 μm. (D) Western blot analysis of MuRF1, Atrogin-1, FoxO3a, p-AKT (Ser473), and total AKT in the soleus muscle of control, HU, and HU+TUDCA mice (n = 6). MW, molecular weight. Data are shown as the mean ± SD. *$p < 0.05$, **$p < 0.01$, ***$p < 0.001$ vs. the control (Con) group; #$p < 0.05$, ##$p < 0.01$, ###$p < 0.001$ vs. the HU group by one-way analysis of variance.

3.4 ER Stress is Activated in HDBR-Induced Muscle Atrophy

Finally, ER stress was measured in atrophied primate muscle caused by disuse. Rhesus macaques were subjected to 42 days of –10° HDBR to induce muscle atrophy. HDBR resulted in a 44.7% decrease in the soleus muscle myofiber CSA (Fig. 4A), which was accompanied by increased expression of both the atrophy-related gene *Fbxo30* and glycolytic myofiber isoform *MyHC-IIb* (Fig. 4B,C). Regarding ER stress markers, *ATF6* and *ATF4* mRNA levels were increased by HDBR, whereas other genes remained unchanged (Fig. 4D). At the protein level, phospho-IRE1α (S724) (p-IRE1α), ATF4, and CHOP were significantly elevated in response to HDBR (Fig. 4E). Importantly, correlation analysis confirmed that the relative expression of both ATF4 and CHOP was positively correlated with the loss of myofiber CSA in atrophied muscles (Fig. 4F), indicating that ER stress activation may play an essential role in disuse-induced primate muscle atrophy.

4. Discussion

Loss of skeletal muscle mass, commonly referred to as muscle atrophy or wasting, results from various physiological and pathological conditions such as disuse, aging, cancer, diabetes, inflammation, and starvation [1–4]. Skeletal muscle atrophy not only leads to muscle weakness and compromises quality of life but also increases the risk of both morbidity and mortality in numerous pathologies. Thus, the development of treatments to combat skeletal muscle atrophy is essential for the maintenance of human health [1–4]. However, a comprehensive understanding of the molecular mechanisms of skeletal muscle atrophy has not been fully

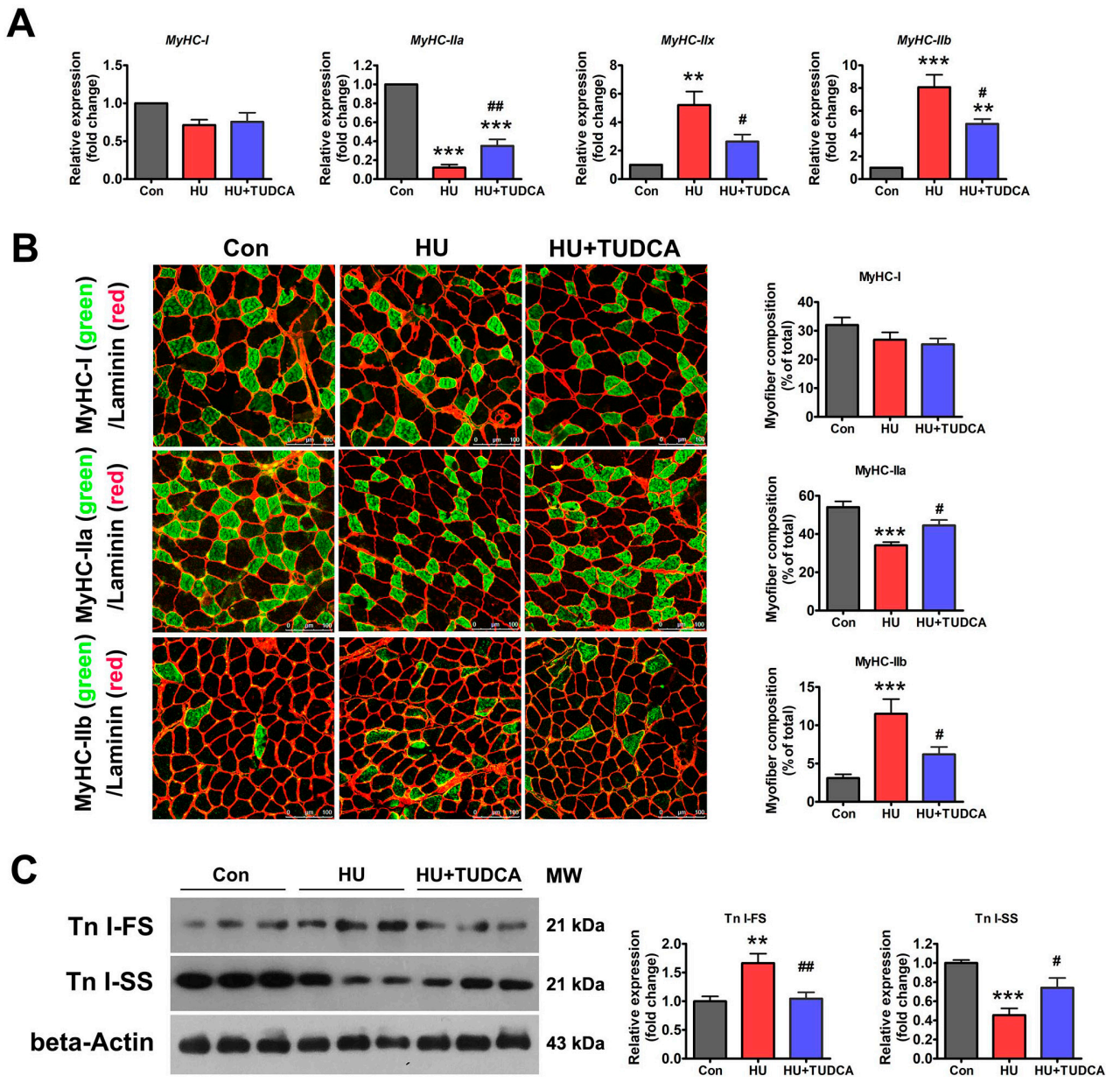

Fig. 3. TUDCA inhibited the oxidative-to-glycolytic myofiber type transition induced by HU. (A) qPCR analysis of *MyHC* isoforms in the soleus muscle of control, HU and HU+TUDCA mice (n = 5). (B) Representative immunostaining of different MyHC isoforms in combination with anti-laminin in the soleus muscle cross-sections of control, HU and HU+TUDCA mice and quantification of the myofiber composition (n = 6). Scale bars: 100 μm. (C) Western blot analysis of Tn I-SS and Tn I-FS in the soleus muscle of control, HU, and HU+TUDCA mice (n = 6). MW: molecular weight. Data are shown as the mean ± SD. $^{**}p < 0.01$, $^{***}p < 0.001$ vs. the control (Con) group; $\#p < 0.05$, $\#\#p < 0.01$ vs. the HU group by one-way analysis of variance.

defined, which has somewhat hindered the development of effective treatments for muscle atrophy.

Over the past decade, studies have increasingly recognized the importance of ER stress and UPR in the regulation of muscle mass [11]. ER stress and UPR are activated in most wasting disorders induced by various stimuli including starvation, sarcopenia, cancer cachexia, denervation, and myopathies [9]. However, research on the expression of ER stress markers during disuse-induced muscle atrophy remains controversial [15,17,24]. For example, an early study reported no significant changes in the expression of UPR markers such as BiP, calreticulin, CHOP, and eIF2α in skeletal muscle in response to inactivity [15]. Another study also showed that 14 days of HU had no effect on the expression of BiP and CHOP in both adult and old rat skeletal muscles [16]. However, *ATF4*, a downstream transcription factor of PERK, is elevated in denervated skeletal muscle [24]. ER stress markers including *ATF4*, *CHOP*, *BiP*, and *Xbp1s* are reportedly upregulated in the gastrocnemius muscle of mice exposed to HU [17].

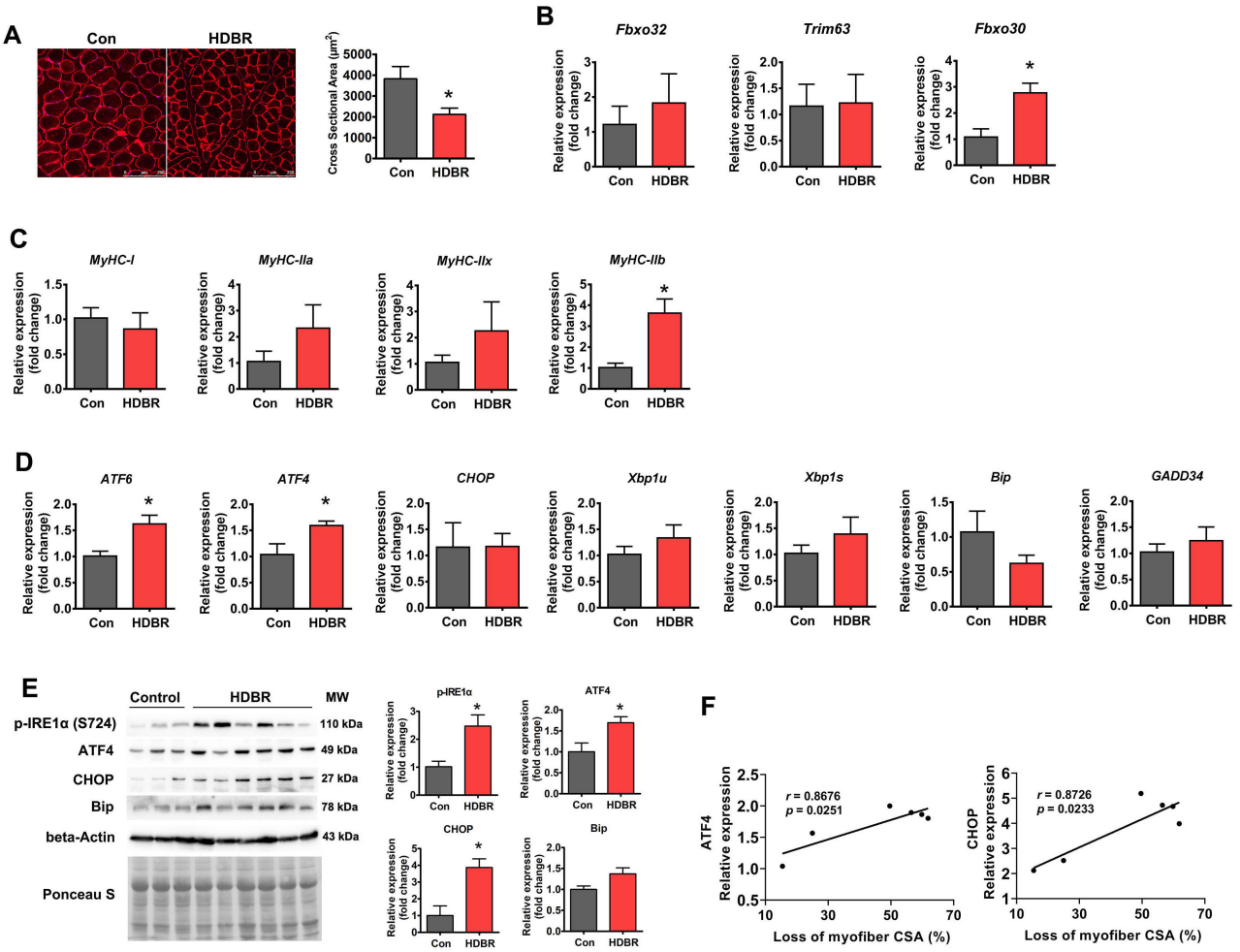

Fig. 4. ER stress was activated in HDBR-induced muscle atrophy. (A) Representative immunostaining for laminin in the soleus muscle cross-sections from rhesus macaques with (HDBR) or without (Con) HDBR and quantification of CSA. Scale bars: 250 μm. (B) qPCR analysis of atrophy-related genes in the soleus muscle of Con and HDBR rhesus macaques. (C) qPCR analysis of *MyHC* isoforms in the soleus muscle of Con and HDBR rhesus macaques. (D) qPCR analysis of the indicated ER stress marker genes in the soleus muscle of Con and HDBR rhesus macaques. (E) Western blot analysis of p-IRE1α (S724), ATF4, CHOP, and BiP in the soleus muscle of Con and HDBR rhesus macaques. MW, molecular weight. (F) Correlation between the expression of ER stress marker proteins and loss of soleus myofiber CSA. Regression lines are displayed. r, correlation coefficient. Pearson's correlation analysis was used to determine significant correlations. (Con, n = 3; HDBR, n = 6). Data are shown as the mean ± SD. *$p < 0.05$ vs. the control group by the *t*-test.

To gain a clear overview of ER stress activation that occurs during progression of muscle atrophy, the expression of ER stress markers was examined in the soleus muscle of mice subjected to different periods of HU. The results of the current study showed the significant upregulation of most ER stress markers, specifically components of the PERK and IRE1α arms, within the first week of HU. By contrast, most ER stress markers (except *ATF6* and *ATF4*) remained unchanged in rhesus soleus muscle upon HDBR, which is not surprising because peak upregulation of gene expression may be missed after 42 days of disuse. Thus, the rapid induction of ER stress markers during the early stage of disuse is consistent with the hypothesis that a major physiological role of the abundant ER in skeletal muscle is to endow the muscle with a rapid response to environmental changes.

The protein expression of ER stress markers was not too low to be detected in mouse soleus muscle, but we successfully detected the protein expression of ER stress markers in primate muscles at basic physiological levels and found that ER stress was activated during HDBR-induced muscle atrophy. Furthermore, correlation analysis showed a positive correlation between ER stress and both HU- and HDBR-induced muscle atrophy, indicating that the activation of ER stress is ubiquitously involved in disuse-induced muscle atrophy, regardless of species.

TUDCA is one of the most commonly used pan-inhibitors of ER stress, which acts as a chemical chaperone to alleviate ER stress and UPR by stabilizating improperly folded proteins [25]. To confirm the involvement of ER stress in disuse-induced muscle atrophy, mice were treated

with TUDCA to block ER stress activation in response to muscle disuse. ER stress inhibition with TUDCA attenuated the muscle atrophy and myofiber type transition caused by HU, indicating that ER stress activation contributes to disuse-induced muscle atrophy. In agreement with these results, overexpression of ATF4 has been found to be sufficient to induce muscle atrophy by inhibiting global protein synthesis [26], and targeted knockout of the *ATF4* gene in skeletal muscle partially prevents acute muscle atrophy during fasting and disuse [26,27]. By contrast, ER stress is activated in cachexia-induced muscle atrophy, and inhibition of ER stress with 4-phenyl butyric acid (another pan-ER stress inhibitor) aggravates the loss of muscle mass caused by cachexia [13], indicating that ER stress plays distinct roles in different types of muscle atrophy. We could not rule out the possibility that this discrepancy may result from different ER stress inhibitors used in these two different models, but it is more likely that ER stress may crosstalk with distinct signaling pathways that regulate muscle mass in different types of muscle atrophy. Indeed, in the muscle of Lewis lung carcinoma (LLC)-bearing mice, p-AKT was not altered, whereas phosphorylated mammalian target of rapamycin (p-mTOR) was significantly reduced [13]. Additionally, inhibition of ER stress in LLC-bearing mice further reduced p-mTOR [13]. However, p-mTOR was not altered in disuse-induced muscle atrophy [28], whereas p-Akt was reduced, and its downstream target, FoxO3a, was increased in unloaded muscles, as was also shown in this study. Inhibition of ER stress with TUDCA reversed HU-induced changes in the expression of p-AKT and FoxO3a in unloaded muscles. Thus, it is plausible that induction of ER stress activation by various atrophic stimuli may result in different outputs by interacting with distinct signaling pathways.

One limitation of this study is that we did not determine the role of ER stress in the atrophy of other hindlimb muscles (such as the gastrocnemius muscle) induced by disuse. Although the atrophy of the gastrocnemius muscle occurs to a relatively lesser extent than that of the soleus muscle during HU, this muscle still shows a significant loss of muscle mass under disuse conditions. Whether ER stress is activated and contributes to the loss of gastrocnemius muscle mass needs to be investigated in future studies. Interestingly, ER stress was activated during the recovery process following disuse and showed different expression patterns between young and aged skeletal muscle [18]. Whether this discrepancy is associated with differences in the speed of recovery in young and aged skeletal muscle also warrants further study [16]. The second limitation of this study is that we performed expreiments only in male animals. Recent research have begun to determine whether sex difference affect muscle response to disuse conditions. One study reported that male rats experience greater muscle atrophy in response to HU than females [29], but another study come the opposite conclusion that female rats showed greater loss of muscle mass than males in response to HU [30]. Therefore, whether sex could influence different muscle response to disuse still remain controversial. Whether ER stress is differentially activated in male and female mice and whether TUDCA also display protective effects on female muscle atrophy upon HU deserve further investigation in our future research. The third limitation of this study is that the underlying mechanisms that trigger ER stress during disuse conditions are still unclear, but we speculate that this may be for the following reasons. The first may be the disturbance in calcium homeostasis. Previous studies have confirmed that during disuse, the cytosolic free calcium concentration is elevated [31], and endogenous ER calcium content in myofibers is decreased [32]. Of note, when calcium levels are lowered in the ER (such as caused by thapsigargin), calcium-dependent ER chaperones lose their chaperone activity, leading to the accumulation of unfolded proteins and UPR [33]. Therefore, in disuse-induced muscle atrophy, the decreased concentration of calcium in the ER may also lead to the accumulation of unfolded proteins and ER stress. Second, ER stress may be secondary to oxidative stress. It has been reported that oxidative stress disrupts ER homeostasis and activates ER stress [34]. Given that reactive oxygen species (ROS) production is increased in disuse-induced muscle atrophy [35], it is intriguing to determine whether ROS induced by disuse contributes to the activation of ER stress in atrophied muscle. Third, the accumulation of fatty acids may contribute to ER stress. The capacity to oxidize long-chain fatty acids in skeletal muscle is significantly reduced in rats after 9 days of spaceflight [36]. Pagano [37] also observed that 3 days of dry immersion promotes fatty acid infiltration into the skeletal muscle of healthy adult men. As saturated fatty acids, especially palmitate, can induce ER stress in a variety of cells including skeletal muscle [38], the accumulation of palmitate in skeletal muscle during disuse may also be a potential factor triggering ER stress. The above-mentioned factors may not be sufficient to induce ER stress activation alone, but the combined action of these factors makes it possible.

5. Conclusions

Collectively, our results provide clear evidence that ER stress is involved in disuse-induced muscle atrophy. Particularly, the high expression of ER stress markers at basic physiological levels in primate muscles and their significant upregulation during HDBR-induced muscle atrophy suggest that ER stress may play a more pronounced role in muscle atrophy in humans than in mice. Pan-inhibition of ER stress with TUDCA represents an attractive therapeutic strategy for disuse muscle atrophy. It has also shown efficacy and tolerability in patients with amyotrophic lateral sclerosis [39]. Moreover, if we translate TUDCA dosage from mice to humans by using the body surface area normalization method [40], the dose used in this study is

equivalent to that has been used in humans [39,41]. Thus, TUDCA has great potential for the treatment of muscle atrophy in individuals suffering from long-term disuse such as bedrest, denervation, or aging.

Abbreviations

ATF, activating transcription factor; BiP, binding immunoglobulin protein; CHOP, C/EBP homologous protein; eIF2, eukaryotic initiation factor 2; ER, endoplasmic reticulum; FoxO3a, forkhead box O3a; HDBR, head-down tilted bed rest; HU, hindlimb unloading; IRE1, inositol requiring enzyme 1; MuRF1, muscle RING finger 1; MUSA1, muscle ubiquitin ligase of SCF complex in atrophy-1; MyHC, myosin heavy chain; PERK, PKR-like endoplasmic reticulum kinase; qPCR, quantitative PCR; TUDCA, tauroursodeoxycholic acid; UPR, unfolded protein response; XBP1s, X-box binding protein 1 spliced; XBP1u, X-box binding protein 1 unspliced.

Availability of Data and Materials

The datasets used and/or analyzed during the current study are available from the corresponding author on reasonable request.

Author Contributions

PZ and XC designed the research study. LW, XP, SL, and WL performed the research. LW, XP and PZ analyzed the data. PZ, LW, XP and XC wrote the manuscript. All authors contributed to editorial changes in the manuscript. All authors read and approved the final manuscript.

Ethics Approval and Consent to Participate

All experiments involving animals were conducted in accordance with standard ethical guidelines and approved by the Institutional Animal Care and Use Committee of China Astronaut Research and Training Center (Approval: ACC-IACUC-2021-021 for mice experiments and ACC-IACUC-2019-002 for rhesus experiments).

Acknowledgment

Not applicable.

Funding

This work was supported by grants from the National Natural Science Foundation of China (81871522, 32171173) and the State Key Laboratory Grant of Space Medicine Fundamentals and Application (SMFA18B01, SMFA20A02).

Conflict of Interest

The authors declare no conflict of interest.

Supplementary Material

Supplementary material associated with this article can be found, in the online version, at https://doi.org/10.31083/j.fbl2807136.

References

[1] Mukund K, Subramaniam S. Skeletal muscle: A review of molecular structure and function, in health and disease. Wiley Interdisciplinary Reviews. Systems Biology and Medicine. 2020; 12: e1462.

[2] Nunes EA, Stokes T, McKendry J, Currier BS, Phillips SM. Disuse-induced skeletal muscle atrophy in disease and nondisease states in humans: mechanisms, prevention, and recovery strategies. American Journal of Physiology. Cell Physiology. 2022; 322: C1068–C1084.

[3] Lee PHU, Chung M, Ren Z, Mair DB, Kim DH. Factors mediating spaceflight-induced skeletal muscle atrophy. American Journal of Physiology. Cell Physiology. 2022; 322: C567–C580.

[4] Hardy EJO, Inns TB, Hatt J, Doleman B, Bass JJ, Atherton PJ, *et al*. The time course of disuse muscle atrophy of the lower limb in health and disease. Journal of Cachexia, Sarcopenia and Muscle. 2022; 13: 2616–2629.

[5] Zhang SS, Zhou S, Crowley-McHattan ZJ, Wang RY, Li JP. A Review of the Role of Endo/Sarcoplasmic Reticulum-Mitochondria Ca^{2+} Transport in Diseases and Skeletal Muscle Function. International Journal of Environmental Research and Public Health. 2021; 18: 3874.

[6] Marafon BB, Pinto AP, Ropelle ER, de Moura LP, Cintra DE, Pauli JR, *et al*. Muscle endoplasmic reticulum stress in exercise. Acta Physiologica (Oxford, England). 2022; 235: e13799.

[7] Lemmer IL, Willemsen N, Hilal N, Bartelt A. A guide to understanding endoplasmic reticulum stress in metabolic disorders. Molecular Metabolism. 2021; 47: 101169.

[8] Maurel M, Chevet E. Endoplasmic reticulum stress signaling: the microRNA connection. American Journal of Physiology. Cell Physiology. 2013; 304: C1117–26.

[9] Gallot YS, Bohnert KR. Confounding Roles of ER Stress and the Unfolded Protein Response in Skeletal Muscle Atrophy. International Journal of Molecular Sciences. 2021; 22: 2567.

[10] Afroze D, Kumar A. ER stress in skeletal muscle remodeling and myopathies. The FEBS Journal. 2019; 286: 379–398.

[11] Bohnert KR, McMillan JD, Kumar A. Emerging roles of ER stress and unfolded protein response pathways in skeletal muscle health and disease. Journal of Cellular Physiology. 2018; 233: 67–78.

[12] Wu J, Ruas JL, Estall JL, Rasbach KA, Choi JH, Ye L, *et al*. The unfolded protein response mediates adaptation to exercise in skeletal muscle through a PGC-1α/ATF6α complex. Cell Metabolism. 2011; 13: 160–169.

[13] Bohnert KR, Gallot YS, Sato S, Xiong G, Hindi SM, Kumar A. Inhibition of ER stress and unfolding protein response pathways causes skeletal muscle wasting during cancer cachexia. FASEB Journal. 2016; 30: 3053–3068.

[14] Marzuca-Nassr GN, Kuwabara WMT, Vitzel KF, Murata GM, Torres RP, Mancini-Filho J, *et al*. Endoplasmic Reticulum Stress and Autophagy Markers in Soleus Muscle Disuse-Induced Atrophy of Rats Treated with Fish Oil. Nutrients. 2021; 13: 2298.

[15] Hunter RB, Mitchell-Felton H, Essig DA, Kandarian SC. Expression of endoplasmic reticulum stress proteins during skeletal muscle disuse atrophy. American Journal of Physiology. Cell Physiology. 2001; 281: C1285–90.

[16] Baehr LM, West DWD, Marcotte G, Marshall AG, De Sousa LG, Baar K, *et al*. Age-related deficits in skeletal muscle recovery following disuse are associated with neuromuscular junction

instability and ER stress, not impaired protein synthesis. Aging. 2016; 8: 127–146.
[17] Azeem M, Qaisar R, Karim A, Ranade A, Elmoselhi A. Signature molecular changes in the skeletal muscle of hindlimb unloaded mice. Biochemistry and Biophysics Reports. 2021; 25: 100930.
[18] Zhang P, Li W, Liu H, Li J, Wang J, Li Y, *et al*. Dystrophin involved in the susceptibility of slow muscles to hindlimb unloading via concomitant activation of TGF-β1/Smad3 signaling and ubiquitin-proteasome degradation in mice. Cell Biochemistry and Biophysics. 2014; 70: 1057–1067.
[19] Chen X, Wang J, Gao X, Wu Y, Gu G, Shi M, *et al*. Tauroursodeoxycholic acid prevents ER stress-induced apoptosis and improves cerebral and vascular function in mice subjected to subarachnoid hemorrhage. Brain Research. 2020; 1727: 146566.
[20] Ozcan U, Yilmaz E, Ozcan L, Furuhashi M, Vaillancourt E, Smith RO, *et al*. Chemical chaperones reduce ER stress and restore glucose homeostasis in a mouse model of type 2 diabetes. Science (New York, N.Y.). 2006; 313: 1137–1140.
[21] Yang JS, Kim JT, Jeon J, Park HS, Kang GH, Park KS, *et al*. Changes in hepatic gene expression upon oral administration of taurine-conjugated ursodeoxycholic acid in ob/ob mice. PLoS ONE. 2010; 5: e13858.
[22] Van den Bossche L, Hindryckx P, Devisscher L, Devriese S, Van Welden S, Holvoet T, *et al*. Ursodeoxycholic Acid and Its Taurine- or Glycine-Conjugated Species Reduce Colitogenic Dysbiosis and Equally Suppress Experimental Colitis in Mice. Applied and Environmental Microbiology. 2017; 83: e02766–16.
[23] Zong B, Wang Y, Wang J, Zhang P, Kan G, Li M, *et al*. Effects of long-term simulated microgravity on liver metabolism in rhesus macaques. FASEB Journal. 2022; 36: e22536.
[24] Sacheck JM, Hyatt JPK, Raffaello A, Jagoe RT, Roy RR, Edgerton VR, *et al*. Rapid disuse and denervation atrophy involve transcriptional changes similar to those of muscle wasting during systemic diseases. FASEB Journal. 2007; 21: 140–155.
[25] Kusaczuk M. Tauroursodeoxycholate-Bile Acid with Chaperoning Activity: Molecular and Cellular Effects and Therapeutic Perspectives. Cells. 2019; 8: 1471.
[26] Fox DK, Ebert SM, Bongers KS, Dyle MC, Bullard SA, Dierdorff JM, *et al*. p53 and ATF4 mediate distinct and additive pathways to skeletal muscle atrophy during limb immobilization. American Journal of Physiology. Endocrinology and Metabolism. 2014; 307: E245–E261.
[27] Ebert SM, Dyle MC, Kunkel SD, Bullard SA, Bongers KS, Fox DK, *et al*. Stress-induced skeletal muscle Gadd45a expression reprograms myonuclei and causes muscle atrophy. The Journal of Biological Chemistry. 2012; 287: 27290–27301.
[28] Chen J, Li Z, Zhang Y, Zhang X, Zhang S, Liu Z, *et al*. Mechanism of reduced muscle atrophy via ketone body (D)-3-hydroxybutyrate. Cell & Bioscience. 2022; 12: 94.
[29] Mortreux M, Rosa-Caldwell ME, Stiehl ID, Sung DM, Thomas NT, Fry CS, *et al*. Hindlimb suspension in Wistar rats: Sex-based differences in muscle response. Physiological Reports. 2021; 9: e15042.
[30] Yoshihara T, Natsume T, Tsuzuki T, Chang SW, Kakigi R, Sugiura T, *et al*. Sex differences in forkhead box O3a signaling response to hindlimb unloading in rat soleus muscle. The Journal of Physiological Sciences: JPS. 2019; 69: 235–244.
[31] Hu NF, Chang H, Du B, Zhang QW, Arfat Y, Dang K, *et al*. Tetramethylpyrazine ameliorated disuse-induced gastrocnemius muscle atrophy in hindlimb unloading rats through suppression of Ca^{2+}/ROS-mediated apoptosis. Applied Physiology, Nutrition, and Metabolism. 2017; 42: 117–127.
[32] Lamboley CR, Wyckelsma VL, Perry BD, McKenna MJ, Lamb GD. Effect of 23-day muscle disuse on sarcoplasmic reticulum Ca2+ properties and contractility in human type I and type II skeletal muscle fibers. Journal of Applied Physiology (Bethesda, Md.: 1985). 2016; 121: 483–492.
[33] Oslowski CM, Urano F. Measuring ER stress and the unfolded protein response using mammalian tissue culture system. Methods in Enzymology. 2011; 490: 71–92.
[34] Katseff A, Alhawaj R, Wolin MS. Redox and Inflammatory Signaling, the Unfolded Protein Response, and the Pathogenesis of Pulmonary Hypertension. Advances in Experimental Medicine and Biology. 2021; 1304: 333–373.
[35] Gao Y, Arfat Y, Wang H, Goswami N. Muscle Atrophy Induced by Mechanical Unloading: Mechanisms and Potential Countermeasures. Frontiers in Physiology. 2018; 9: 235.
[36] Baldwin KM, Herrick RE, McCue SA. Substrate oxidation capacity in rodent skeletal muscle: effects of exposure to zero gravity. Journal of Applied Physiology (Bethesda, Md.: 1985). 1993; 75: 2466–2470.
[37] Pagano AF, Brioche T, Arc-Chagnaud C, Demangel R, Chopard A, Py G. Short-term disuse promotes fatty acid infiltration into skeletal muscle. Journal of Cachexia, Sarcopenia and Muscle. 2018; 9: 335–347.
[38] Woodworth-Hobbs ME, Perry BD, Rahnert JA, Hudson MB, Zheng B, Russ Price S. Docosahexaenoic acid counteracts palmitate-induced endoplasmic reticulum stress in C2C12 myotubes: Impact on muscle atrophy. Physiological Reports. 2017; 5: e13530.
[39] Albanese A, Ludolph AC, McDermott CJ, Corcia P, Van Damme P, Van den Berg LH, *et al*. Tauroursodeoxycholic acid in patients with amyotrophic lateral sclerosis: The TUDCA-ALS trial protocol. Frontiers in Neurology. 2022; 13: 1009113.
[40] Reagan-Shaw S, Nihal M, Ahmad N. Dose translation from animal to human studies revisited. FASEB Journal. 2008; 22: 659–661.
[41] Falasca L, Tisone G, Palmieri G, Anselmo A, Di Paolo D, Baiocchi L, *et al*. Protective role of tauroursodeoxycholate during harvesting and cold storage of human liver: a pilot study in transplant recipients. Transplantation. 2001; 71: 1268–1276.